Adsorption, 1, 203–211 (1995)

Effect of Variable Feed Concentration on the Performance of a Pressure Swing Adsorption Process

RAVI KUMAR*
Air Products and Chemicals, Inc., 7201 Hamilton Boulevard, Allentown, PA 18195-1501

Abstract. Effects of variable feed composition on the performance of a pressure swing adsorption process are analyzed by simulation. Two scenarios are considered. The first, "increasing impurity," case considers low impurity concentration in the feed followed by high impurity concentration in the feed. The second, "decreasing impurity," case considers high impurity concentration in the feed followed by low impurity concentration in the feed. These results are compared against a case which has an impurity concentration in the feed at an average of the high and the low impurity concentrations. Simulations show that the increasing impurity scenario is expected to perform better, and the decreasing impurity scenario is expected to perform worse than the average feed concentration case.

Keywords: simulation, pressure swing adsorption, fixed bed system, bulk separation

Introduction

Pressure swing adsorption (PSA) processes are extensively used in the industry to achieve desired separation and purification (Ruthven, Farooq and Knaebel, 1994; Ruthven, 1984). Some examples of these processes are production of Hydrogen from refinery off-gases and production of carbon monoxide from SMR off gas, etc. PSA's are usually located downstream of a process which provides the feed mixture to the PSA. Therefore, in some instances, composition of the feed to the PSA varies with time. The most common approach to handle these variations is to install a mixing vessel upstream of the PSA and design the adsorption system based upon the average feed composition. In addition, multitrain PSA processes (Kumar, 1990; Kumar and Kratz, 1992) produce an effluent from the first train which has a variable composition of the impurities being fed to the second or the downstream PSA train. In such instances a mixing vessels is installed between the trains. In the present study, the effects of directly feeding the variable composition feed to a PSA system are examined. This is accomplished by simulating a typical Hydrogen PSA process using a computer model. Details of the computer model were previously published along with experimental data validating this model (Kumar et al, 1994).

*Current Address: The BOC Group, 460 Mountain Avenue, Murray Hill, NJ 07974.

Process Cycle and Simulation

A nine step, four bed PSA cycle to produce high purity hydrogen from a feed mixture containing an average of 25% methane and 75% hydrogen is simulated (Batta, 1971). The process steps are:

1. Feed,
2. First Cocurrent Depressurization,
3. Second Cocurrent Depressurization,
4. Third Cocurrent Depressurization,
5. Blowdown by Countercurrent Depressurization,
6. Countercurrent Purge by Gas from Step 3,
7. First Product/Product Pressure Equalization,
8. Second Product/Product Pressure Equalization, and
9. Product Repressurization.

The time chart for the process is illustrated in Fig. 1. The process simulator uses only one bed to simulate all the four beds of the process (Kumar et al., 1994). To describe the bed connectivities, temporal effluent arrays (flow, pressure, composition, and temperature) from a process step are retained and used later when the bed is undergoing the appropriate process step. Figure 2 depicts the manner in which the above cycle is simulated (Kumar, 1994).

The model equations are summarized in the appendix and the simulation parameters are listed in Table 1. Three sets of simulations were carriedout in the present study. For the first set, base case, feed composition was set at 25% methane and 75% hydrogen for the entire

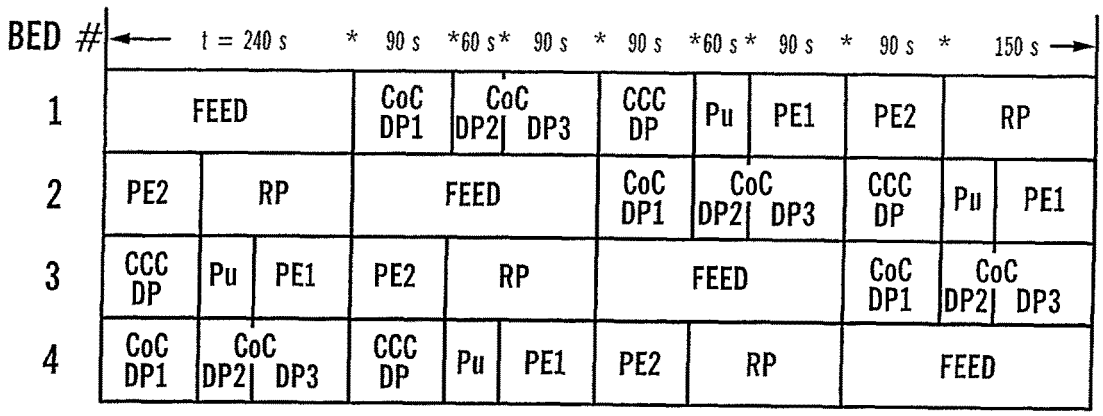

Fig. 1. Time chart for the simulated process. CoCDP1—First cocurrent depressurization to provide first pressure equalization (PE1) gas, CoCDP2—Second cocurrent depressurization to provide purge (Pu) gas, CoCDP3—Third cocurrent depressurization to provide second pressure equalization (PE2) gas, CCCDP—countercurrent depressurization or blowdown to low pressure, RP—product repressurization to feed pressure.

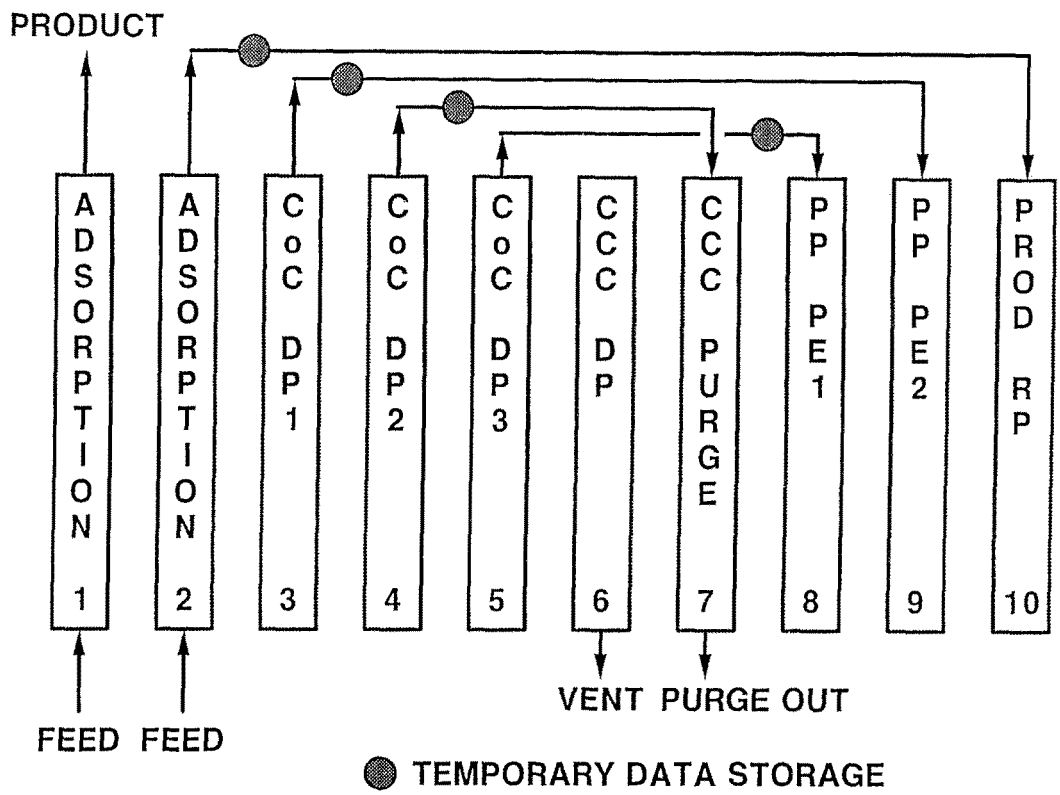

Fig. 2. Simulation break up for the four bed pressure swing adsorption process to produce hydrogen.

240 s duration of the feed step. The process was optimized to achieve high purity hydrogen (Kumar, 1994). The second set of simulations, cases #1 and 2, had low methane concentration in the feed for the first 120 s followed by high methane concentration in the feed for the last 120 s such that the average methane concentration in the feed methane was 25%. Case #1 had 12.5% methane for the first 120 s and 37.5% methane for the last 120 s. Case #2 had 5% methane for the last 120 s and 45% methane for the last 120 s. The balance of

Table 1. Simulation parameters.

	Simulation parameters		
Adsorbent:	Ca exchanged A zeolite, 1/16″ pellets		
	Particle diameter	=	0.0053 ft
	Bulk density	=	46.21 lb/ft^3, as packed
	Heat capacity	=	0.22 Btu/lb/°F
Feed gas:	H_2-average	=	75%
	CH_4-average	=	25%
	Temperature	=	25°C
Column:	Inside diameter	=	0.93 inch
	Column length	=	20 ft
	Adsorbent void fraction	=	0.700
	Interstitial void fraction	=	0.380
	Gas to wall heat transfer coefficient	=	0.005 Btu/hr/ft^2/°F
	Equilibrium parameters		
	Adsorbent: Ca exchanged zeolite A		
Adsorbate:	CH_4		H_2
m-mmole/gm	1.51		
$b°$, atm^{-1}	9.38×10^{-5}		4.68×10^{-4}
q, cal/gmole	5,347		2,069
	Mass transfer coefficient		
		k_i = PFACi/P	
	CH_4		H_2
PFAC, atm/s	4.8		194

the feed was hydrogen in the mixture. These are the "increasing impurity" cases.

The third set of simulations, cases #3 and 4, had high methane concentration in the feed for the first 120 s followed by low methane concentration in the feed for the last 120 s such that the average methane concentration in the feed was 25%. Case #3 had 37.5% methane for the first 120 s and 12.5% methane for the last 120 s. Case #4 had 45% methane for the first 120 s and 5% methane for the last 120 s. The balance of the feed was hydrogen in the mixture. These are the "decreasing impurity" cases.

Results and Discussion

For each of the increasing and decreasing impurity cases, two runs were made. The first set of runs, set-a, had the same feed flow rate as the base case. For these cases, the product purity was allowed to vary. The second set of runs, set-b, had roughly the same product purity as the base case. For these cases, the feed flow rate was changed.

Increasing Feed Impurity

Table 2 summarizes the results for these cases. It is observed that for the cases #1a and #2a, for which the feed flow rate is maintained at the same level as the base case, product purity is higher than the base case. Figures 3 and 4, respectively, show the gas phase methane concentration and the solid phase methane loading profiles inside the column at the end of the feed steps for the cases: base, 1a, and 2a. It is observed that as the methane concentration in the feed is increased, in the second-half of the feed step, the portion of the bed initially loaded by lower methane concentration is further loaded to a higher value. Therefore, in this scenario, the feed-end of the bed is used twice. Once to adsorb methane from the lower concentration feed stream and then to adsorb methane on top of the previously adsorbed methane from the higher concentration feed stream. This increased utility of the adsorbent is responsible for the observed higher product purity for these cases.

It is also observed from Figs. 3 and 4 that the leading front of methane concentration and loading is moved

Table 2. Increasing feed impurity—comparative performance.

Case	Feed CH_4 (%)	Product CH_4 (PPM)	H_2 recovery (%)	Fresh feed (mlbmole/lb)	Product H_2 (mlbmole/lb)
Base	25% for 240 s	4	84.5	1.94	1.24
1a	12.5% for 120 s and	0	84.7	1.95	1.24
1b	37.5% for 120 s	3	87.4	2.13	1.40
2a	5% for 120 s and	0	85.1	1.95	1.24
2b	45% for 120 s	0.1	88.1	2.19	1.45

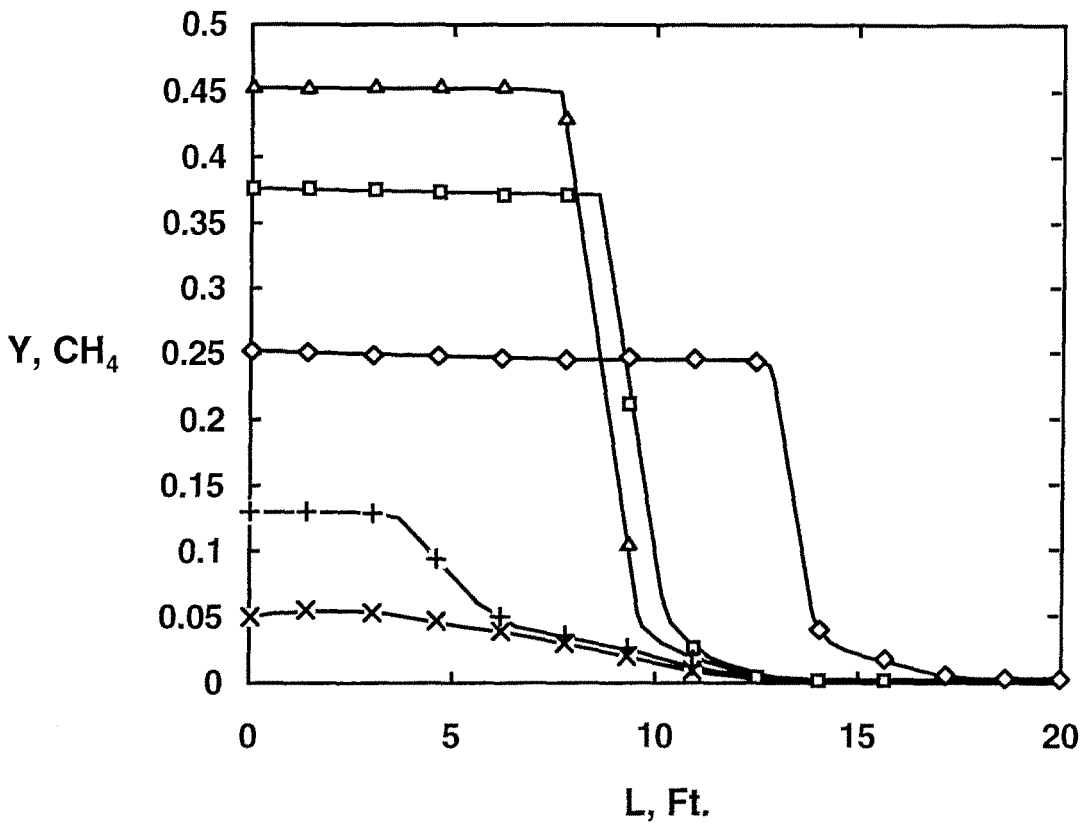

Fig. 3. Methane concentration profiles inside the column at the end of the feed step. ◊, base case, -+-, and --□--: increasing concentration of methane in the feed at 12.5% and 37.5%, respectively, -×- and --△--: increasing concentration of methane in the feed at 5% and 45%, respectively.

farther down the bed for the case when 37.5% methane follows 12.5% methane in the feed (Case #1a, --□- and -+- in Fig. 3) than for the case when 45% methane follows 5% methane in the feed (Case #2a -△- and --×- in Fig. 3). Therefore, it is concluded that for increasing feed impurity cases, farther apart the minimum and the maximum feed concentrations are from an average value, larger is the expected performance improvement from a process designed to handle the average feed composition.

Cases #1b and #2b, for which the product purity was maintained roughly at the same level as the base by increasing the feed flow rate, show higher recovery and increased productivity than the base case. Also, as

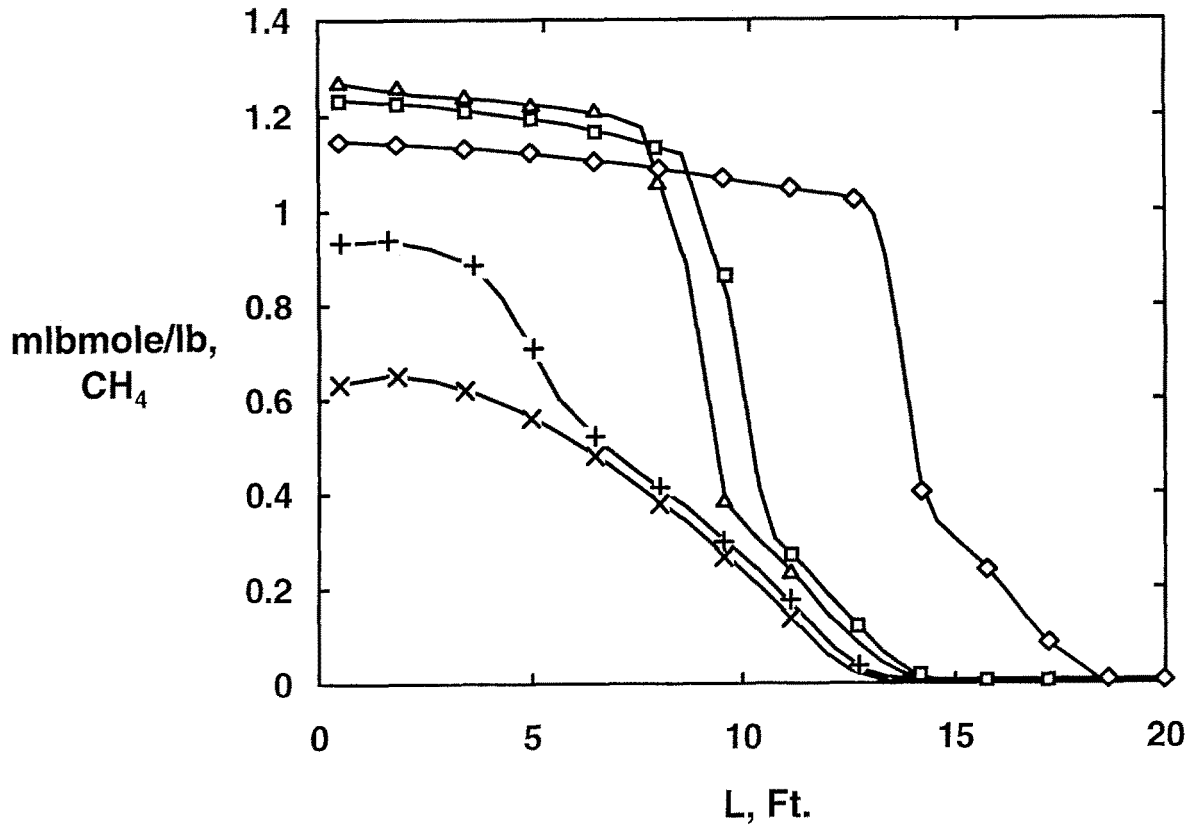

Fig. 4. Methane loading profiles inside the column at the end of the feed step. ◊, base case; -+-, and --□--: increasing concentration of methane in the feed at 12.5% and 37.5%, respectively; -×- and --Δ--: increasing concentration of methane in the feed at 5% and 45%, respectively.

expected from the above discussion, the improvement is higher for Case #2b, 5% methane followed by 45% methane than for Case #1b, 12.5% methane followed by 37.5% methane.

Based upon these observations, one can say that if the feed impurity concentration to a PSA system increases during the feed step, a mixing vessel upstream of the PSA is not necessary. It may, in fact, cause inferior PSA performance.

Decreasing Feed Impurity

Table 3 summarizes the results for the cases when concentration of methane in the feed decreases during the feed step. It is observed that for the cases #3a and #4a, when the feed flow rate is maintained at the same level as the base case, impurity level in the product increases significantly from 4 ppm to 4.4% for Case #3a and to 8.1% for Case #4a. This behavior is opposite of the behavior observed for the increasing feed impurity cases, Table 2. Figures 5 and 6, respectively, show the gas phase methane concentration and the solid phase methane loading profiles inside the column at the end of the feed steps for the cases: base, 3a, and 4a. It is observed that as the lower concentration of the impurity is introduced into the bed during the second-half of the feed step, it displaces the methane already adsorbed on the bed. This is caused by the purging action provided by the lower concentration of the feed gas. It causes the feed-end of the bed, which was at higher methane loadings from the first-half of the feed step, to desorb. The desorbed methane moves down the bed contaminating the product end and causing large decrease in product purity.

In contrast to the increasing impurity scenario, these cases show that farther apart the maximum and minimum impurity concentrations are from the average value, farther the methane front moves down the bed (Figs. 5 and 6). This can be explained by noticing that farther apart the maximum and minimum impurity

Table 3. Decreasing feed impurity—comparative performance.

Case	Feed CH_4 (%)	Product CH_4 (PPM)	H_2 recovery (%)	Fresh feed (mlbmole/lb)	Product H_2 (mlbmole/lb)
Base	25% for 240 s	4	84.5	1.95	1.24
3a	37.5% for 120 s and	4.4%	78.4	1.95	1.20
3b	12.5% for 120 s	32	78.1	1.60	0.94
4a	45% for 120 s and	8.1%	73.4	1.95	1.17
4b	5% for 120 s	42	73.5	1.44	0.79

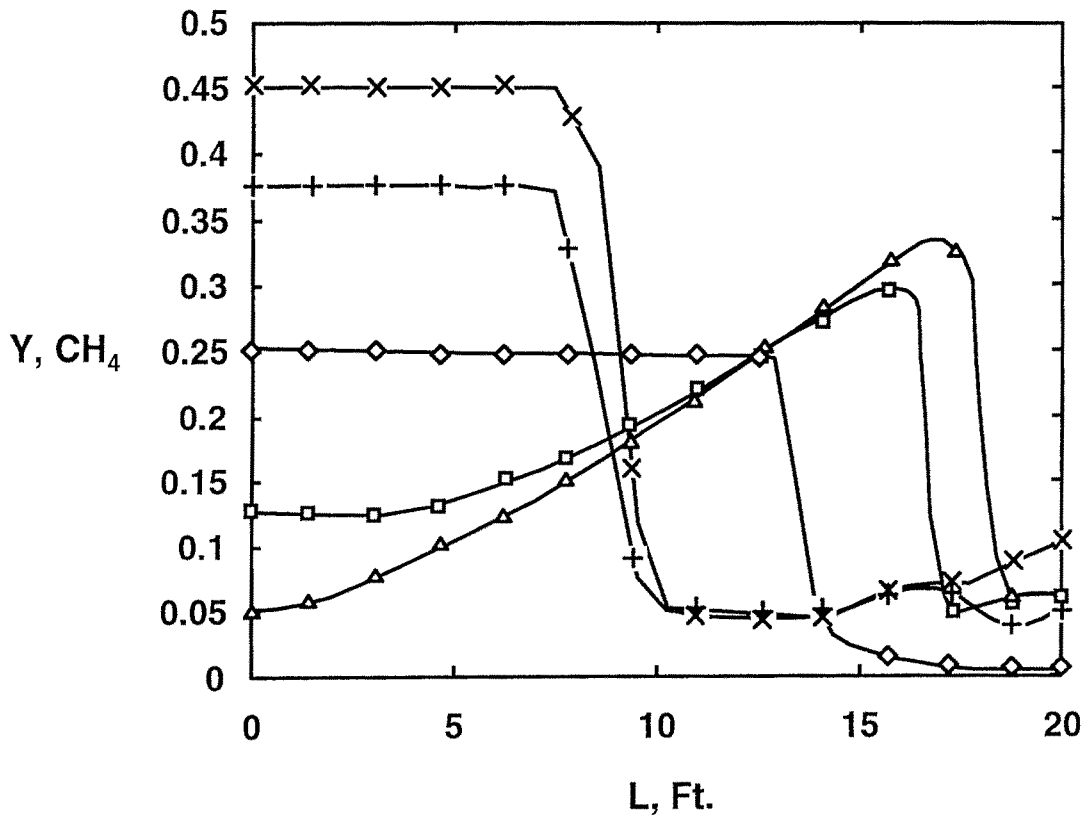

Fig. 5. Methane concentration profiles inside the column at the end of the feed step. ◇, base case, -+-, and - -□- -: decreasing concentration of methane in the feed at 37.5% and 12.5%, respectively; - -×-, and - -Δ- -: decreasing concentration of methane in the feed at 45% and 5%, respectively.

concentrations are from the average value, lower the impurity concentration in the second half of the feed step and therefore better the purging action and thus more desorption of the previously adsorbed methane from the adsorbent. This in turn causes worse performance. It is therefore concluded that for decreasing feed impurity cases, farther apart the minimum and maximum feed concentrations are from an average value, larger the expected performance decline from a process designed to handle the average feed composition.

Cases #3b and #4b, for which the product purity was maintained at roughly the same level as the base case by decreasing the feed flow rate, show lower recovery,

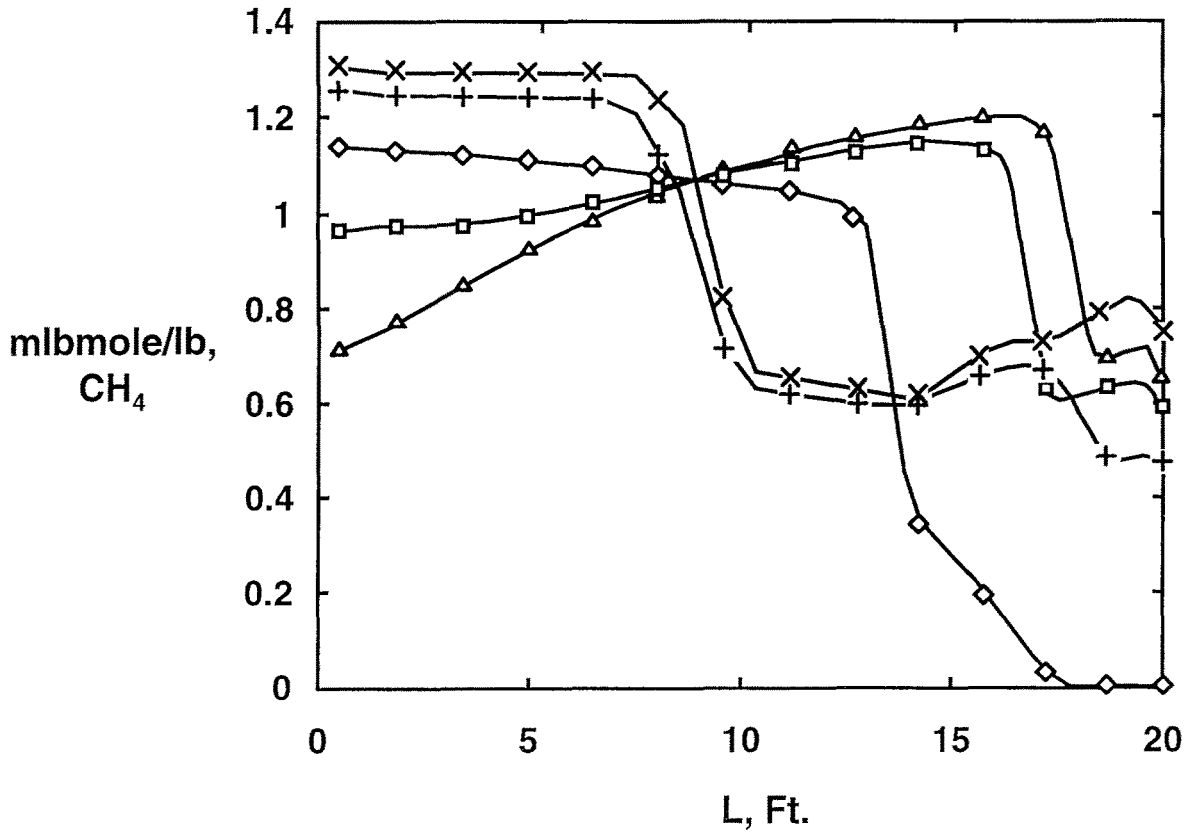

Fig. 6. Methane loading profiles inside the column at the end of the feed step. ◊, base case; -+- and - -□-: decreasing concentration of methane in the feed at 37.5% and 12.5%, respectively; - -×-, and - -Δ- -: decreasing concentration of methane in the feed at 45% and 5%, respectively.

and decreased productivity than the base case. Also, as expected from the above discussion, the decline is higher for Case #4b, 45% methane followed by 5% methane, than for Case #3b, 37.5% methane followed by 12.5% methane.

Based upon these observations, a mixing vessel upstream of the PSA is recommended if the concentration of the impurity in the feed to a PSA is expected to decrease during the feed step.

Variable Feed Impurity

Four simulations were run with variable feed impurity concentration. In contrast to the cases discussed above, for which there was only one step change between the concentration levels, these cases had two or three step changes in the feed composition. The simulation results for these cases are summarized in Table 4.

For Case #5, the methane concentration was first low (12.5%) then high (37.5%) and then low (12.5%)

Table 4. Variable feed impurity—comparative performance.

Fresh feed quantity = 1.95 mlbmole/lb
Average feed composition: Methane = 25%
Hydrogen = 75%

Case	Feed CH_4(%)	Product CH_4 (PPM)	H_2 recovery (%)
Base	25% for 240 s	4	84.5
5	12.5% for 60 s, 37.5% for 120 s, and 12.5% for 60 s	1.6%	81.9%
6	12.5% for 60 s, 37.5% for 60 s, 12.5% for 60 s, and 37.5% for 60 s	0	84.3
7	37.5% for 60 s, 12.5% for 120 s, and 37.5% for 60 s	0	84.4
8	37.5% for 60 s, 12.5% for 60 s, 37.5% for 60 s, and 12.5% for 60 s	1.5%	81.8

such that the average methane concentration in the feed was the same as the base case. This case shows a large increase in the product methane concentration from 4 ppm to 1.6%. The hydrogen recovery is also reduced. Similar behavior is observed for Case #8. For this case, however, the feed concentration started high (37.5%) then went down (12.5%) then went up (37.5%) and then went down again (12.5%). This suggests that the shape of the feed concentration profile at the beginning of the feed step is of less importance than the shape of the feed concentration profile at the end of the feed step. This conclusion is further supported by results for Cases #6 and #7. For these cases, an improvement in process performance is observed due to increase in feed impurities towards the end of the feed step.

These four cases show that if the impurity concentration in the feed goes up towards the end of the feed step, the process performance will be better than expected based upon average feed concentration, and it would be worse if the impurity concentration goes down towards the end of the feed step.

Conclusions

Simulations for a pressure swing adsorption system when concentration of the impurity in the feed changes during the feed step show that:

- If the feed impurity increases during the feed step, process performance will be better than expected based upon average feed composition. Therefore, a feed mixing tank upstream of the PSA will hurt the process performance. Also, larger concentration swing will cause better performance.
- If the feed impurity decreases during the feed step, process performance will be worse than expected based upon average feed composition. Therefore, a feed mixing tank upstream of the PSA will benefit the process. Also, larger concentration swing will cause worse performance.
- Feed impurity composition variation towards the end of the feed step has a larger impact on the process performance than the feed impurity composition variation at the beginning of the step.
- A process with feed impurity going up towards the end of the feed step will perform better than a process with feed impurity going down towards the end of the feed step.

Acknowledgment

The author is thankful to Air Products and Chemicals, Inc. for their permission to publish this work.

Appendix

Details of the mathematical model were previously published (Kumar et al. 1994). In summary, component (i) mass balance:

$$\varepsilon \frac{\partial}{\partial t}(\rho_g y_i) = -\frac{\partial}{\partial x}(v\rho_g y_i) - \rho_b \frac{\partial n_i}{\partial t}$$

Overall mass balance:

$$\varepsilon \frac{\partial}{\partial t}(\rho_g) = -\frac{\partial}{\partial x}(v\rho_g) - \rho_b \sum \frac{\partial n_i}{\partial t}$$

Energy balance:

$$-\frac{\partial}{\partial x}\left(v\rho_g \int C_{Pg} dT\right) + \rho_b \sum q_i \frac{\partial n_i}{\partial t} - \frac{4hw}{D}(T - T_w) = \rho_b \frac{\partial}{\partial t} \int C_{Ps} dT + \varepsilon \frac{\partial}{\partial t} \int \rho_g C_{vg} dT$$

Momentum balance:

$$-\frac{dP}{dx} = \frac{150\,\mu v}{d_p^2} \frac{(1-\varepsilon_i)^2}{\varepsilon_i^3} + 1.75 \rho v^2 \frac{(1-\varepsilon_i)}{d_p \varepsilon_i^3}$$

Langmuir model for equilibrium isotherm:

$$n_i = \frac{m b_i P y_i}{1 + \sum b_i P y_i}$$

$$b_i = b_i^0 \exp(q_i / RT)$$

Linear driving force model for mass transfer:

$$\frac{\partial n_i}{\partial t} = k_i (n_i^* - n_i)$$

The governing PDE's were discretized in space and the resulting system of ODE's was solved using the LSODE integrator from Lawrence Livermore Laboratory. An HP workstation 735 was used for simulations. In the present study, the total 20 ft. length of the column was divided into forty special nodes. The first 10 ft. of the column from the feed end had 10 nodes, the next 5 ft. also had 10 nodes, and the last 5 ft. has 20 nodes. This node division was chosen to minimize computational time while maximizing the accuracy of product purity.

Nomenclature

b	Langmuir parameter
C_{Pg}	$\sum C_{Pgi}(T) \cdot y_i$, heat capacity of the gas phase
C_{Ps}	adsorbent heat capacity
C_{vg}	$\sum C_{vgi}(T) \cdot y_i$, heat capacity of the gas phase
d_p	particle diameter
D	bed diameter
ε	total bed voidage
ε_i	interstitial void fraction
hw	bed to wall heat transfer coefficient
k	mass transfer coefficient
m	monolayer capacity of the adsorbate
n	solid phase loading
P	total pressure
$PFAC$	proportionality parameter for mass transfer coefficient
q	isosteric heat of adsorption
R	gas constant
ρ	gas phase mass density
ρ_b	bulk density of the adsorbent
ρ_g	gas phase molar density
T	system temperature
t	time variable
T_w	wall temperature
μ	viscosity
v	superficial linear velocity
x	distance variable
y	gas phase mole fraction

Subscript

i	component

Superscript

$*$	corresponding equilibrium concentration

References

Batta, L.B., U.S. Patent #3,564,816, February 23, 1971.

Kumar, R., U.S. Patent #4,913,709, Apr. 3, 1990.

Kumar, R., "Pressure Swing Adsorption Process: Performance Optimum and Adsorbent Selection," *I&EC Research*, **33**, 1600 (1994).

Kumar, R., V.G. Fox, D.G. Hartzog, R.E. Larson, Y.C. Chen, P.A. Houghton, and T. Naheiri, "A Versatile Process Simulator for Adsorptive Separations," *Chem. Eng. Sci.*, **49**(18), 3115 (1994).

Kumar, R. and W.C. Kratz, U.S. patent #5,133,785, Jul. 28, 1992.

Ruthven, D.M., *Principles of Adsorption and Adsorption Processes*, John Wiley & Sons, 1984.

Ruthven, D.M., S. Farooq, and K. Knaebel, *Pressure Swing Adsorption*, VCM Publishers, 1994.